ISSN 0006-3509, Biophysics, 2016, Vol. 61, No. 6, pp. 1002–1010. © Pleiades Publishing, Inc., 2016.
Original Russian Text © A.V. Leonidov, 2016, published in Biofizika, 2016, Vol. 61, No. 6, pp. 1208–1218.

COMPLEX SYSTEMS BIOPHYSICS

On Optical Receivers in the Pathway Implicated in Regulating the Human Circadian Rhythm

A. V. Leonidov

Biofizika, Profsoyuznaya ul. 90, Moscow, 117997 Russia
e-mail: avleonidoff@mail.ru

Received September 15, 2015

Abstract—Biological and mathematical grounding was provided for the mechanism that is responsible for the optical radiation-dependent regulation of the human circadian rhythm that involves the well-known retinal photoreceptors, rods and blue-sensitive cones. It was shown that light-sensitive retinal ganglion cells are unable to act as receivers of optical radiation. Two spectral channels involved in regulating the circadian rhythm were observed in the retino-hypothalamic pathway. An analytical expression for the function of the relative spectral circadian efficiency was obtained for Scalculations and mathematical modeling of the human circadian rhythm.

Keywords: retina, cones, rods, spectral sensitivity, ganglion cells, approximation, identification of photodetectors, function of relative spectral circadian efficiency

DOI: 10.1134/S0006350916060117

An increasing number of studies have recently focused on the putative discovery of a new optical radiation receiver (photodetector) (e.g., see [1–8], etc.) in the form of intrinsically photoreceptive retinal ganglion cells (ipRGCs) [9–15].

According to the authors of the discovery, the photodetector receives radiation of the short-wave region of the visible spectrum and converts and transmits signals to the hypothalamic suprachiasmatic nuclei, the pineal gland, and associated neuronal structures to regulate secretion of the hormone melatonin in the pineal gland during the day, the activity of the neuroendocrine system, and, eventually, the circadian activity of the human body [1–3, 8, 16].

The discovery of ipRGCs has been reported based on the results of independent experimental studies [1–3, 8] aimed at determining the shape of the relative circadian spectral efficiency function (RCSEF).

The function, which is hereafter designated $c(\lambda)$, associates the relative (normalized to unity) plasma melatonin concentration, which is a readily measurable marker of circadian activity, with the wavelength of optical radiation that affects the retina. Two RCSEF shapes that are known to date ($c_B(\lambda$ and $c_T(\lambda)$ have independently been obtained in experimental studies by Brainard et al. and Thapan et al. [1–3, 8] and are shown in Fig. 1.

The spectral ranges and the graphic shapes in the low-wave range of the functions $c_B(\lambda)$ and $c_T(\lambda)$ and their regression functions do not coincide with the spectral efficiency function of any known retinal photodetector; both $c_B(\lambda)$ and $c_T(\lambda)$ substantially differ from the relative spectral luminous efficiency function for photopic ($V(\lambda)$) and mesopic ($V'(\lambda)$) vision [17–

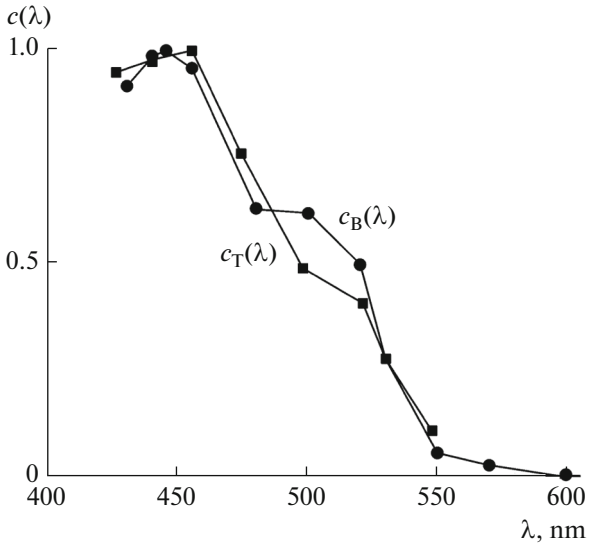

Fig. 1. Experimental plots of the RCSEF $c_B(\lambda)$ [1] and $c_T(\lambda)$ [3].

Abbreviations: ipRGC, intrinsically photoreceptive retinal ganglion cell; RCSEF, relative circadian spectral efficiency function.

19]. The findings indicate that the well-known retinal photodetectors, rods and cones, are not involved in forming the RCSEF. Based on the findings, the hypothesis has been advanced and, more recently, the discovery announced that an earlier unknown photodetector, ipRGCs, exists in the retina.

Physiological studies aimed at verifying the presence of ip RGCs as a photodetector in the retina have been performed in mice. A review of the experimental procedures, their results, and the speculations published to support the idea that ipRGCs are capable of receiving optical radiation make it possible to question some of the conclusions made in [1–3, 8].

As an example, extirpation or genetic modification of the retina has been done to totally eliminate all rods and cones according to the study design described in [1–3, 8]; however, their total elimination has not been achieved [8]. In the experimentally modified mouse retina the remaining rods and cones are capable of transmitting signals on the light environment even via a neuronal network with a changed topology and altered functional connections. Thus, it is principally possible that melatonin secretion and the circadian rhythm are regulated by optical radiation that affects the remaining rods and cones, even when the topology and functional connections of retinal elements are distorted to a substantial extent.

When assuming that it is possible to abolish the functions of all neuronal elements of the retina without affecting the normal function of ganglion cells, it is important to remember that the hypothalamus, which is a leading regulatory element of the neuroendocrine system, has afferent and efferent connections not only with the vision system, but also with other sensory systems of the body. This fact directly indicates that circadian activity may be regulated not only via the retino-hypothalamic pathway, but also via other pathways that transmit information on the status and variation of environmental parameters. For example, the pathway that provides the hypothalamus with information on the variation of environmental temperature during the day may act as such a regulator.

Mice, which were used in the above experiments [1–3, 8], are social animals. When a mouse belongs to a socially isolated group and is exposed to conditions close to light deprivation as a result of extirpation or genetic modification of the retina, its behavior depends to a great extent on the behavior of the other mice of the group. Communications and other relationships among members of a social group lead to a group-level regulation and synchronization of circadian activity in particular members and the total group, especially when the group has been totally isolated from environmental influences for a long period of time. Many examples have been described in the literature to illustrate this regulation of circadian activity and the establishment of a common circadian rhythm in members of an isolated group in the absence of any changes in parameters of the light environment during the day (see [20, 21] and many other works).

These data directly demonstrate that the circadian rhythm can be regulated without involving elements of the vision system. Among other factors, such regulation explains why even blind subjects display relatively stable circadian activity.

Melanopsin, which is contained in ipRGCs, was considered to be a protein that converts optical radiation to neuronal activity in [1–3, 8–15].

The spectral sensitivity in the short-wave range of the visible spectrum and a sensitivity maximum at $\lambda = 440–460$ nm have been ascribed to the protein only on the basis of the positions of the maximums of the functions $c_B(\lambda)$ and $c_T(\lambda)$ (Fig. 1) without any direct experimental verification.

The above circumstances make the interpretation of the results from experimental studies highly questionable and show that caution should be exercised when analyzing and interpreting the experimental findings or stating that retinal ganglion cells act as possible photodetectors in the pathway that regulates circadian activity. Moreover, the above reasoning does not indicate that the so-called ipRGCs govern the relevant processes.

Several other important factors were omitted in [1–3, 8], but may change the ideas on the possible roles that individual elements of the retina play in receiving optical radiation in the pathway that regulates human circadian activity.

Regulation of the human circadian system and its synchronization by optical radiation are possible only when retinal irradiance is sufficiently high (up to several watts per square meter). The quantum properties of optical radiation are negated at these retinal irradiance levels. The spatial and temporal incoherence of radiation from natural sources and the turbulent properties of the channel that serve to propagate optical radiation further negate the quantum properties of optical radiation and cause their statistical averaging [17, 22, 23]. According to the law of large numbers and the central limit theorem of probability theory, characteristics of such radiation flows can be shown as a continuous normal distribution of the probability density. This provides an opportunity to describe the above incoherent radiation flows at the gross level in terms of energy parameters proportional to the optical flow rate, using scalar continuous functions of spatial coordinates and a time coordinate [17, 22, 24, 25]. In other words, the functions are continuous analog signal fields [22–26].

Based on the principles underlying cell activity, cells of the body can be divided into two classes that differ in the nature of signals subject to processing and the signal processing mechanisms.

One class includes evolutionarily ancient cells, which have a low excitation threshold and arose at the

advent of life. These cells receive analog external signals and convert them to analog cell responses at the current evolutionary stage in the same manner that they did in early evolution.

When external influences change monotonically, reversible monotonic changes in cell membrane depolarization are involved in the function of cells with analog signal processing [27–29].

In the case of retinal cells that convert optical radiation to neuronal activity, reversible variations in the extent of cell membrane depolarization arise in response to variations in the spatial, temporal, and energy characteristics of radiation sources; i.e., the cell response to external stimuli is of the analog type [26–29]. Analog-type responses are observed in retinal receptors (rods and three types of cones) and in horizontal and bipolar cells [29].

Cells of the other class arose later in evolution and are capable of far more complex processing and conversion of input signals; their functional role is receiving and processing the input signals and generating binary output signals in the form of spike trains [21]. Analog-to-binary signal conversion occurs in groups of bipolar, amacrine, and ganglion cells in the retina. The cell groups act as analog-to-digital converters [29]. Bipolar cells with analog signal processing are their input elements, and ganglion cells with binary signal processing act as their output elements [21, 27]. Cells with binary signal processing respond to input signals by generating spike trains; i.e., multiple abrupt depolarization events in the cell membrane produce trains of spikes with a constant amplitude and a variable pulse period-to-pulse duration ratio [21, 27, 29]. Amacrine and, importantly, ganglion cells of the retina belong to this class [29].

As in technical information-transmission systems [23], noise resistance and noise protection of signal processing on exposure to variations in external and internal influences are improved as a result of analog-to-binary conversion of neuronal signals in the pathway that regulates human circadian activity.

The following essential conditions must be met to allow a structure, a cell structure in particular, to receive optical radiation.

An obvious condition is that the cell cytoplasm contains a protein that is sensitive to optical radiation [27, 29]. Such proteins undergo reversible denaturation at the secondary or tertiary structure level on exposure to optical radiation varying in spectral composition; this is an analog-type conversion. The condition is met for any protein that occurs in the cytoplasm of any cell given that the spectral range of optical radiation corresponds to the spectral range of sensitivity of the protein in question. The set includes rhodopsin, iodopsin [17, 18, 21, 27, 29], and, certainly, melanopsin found in ganglion cells [8].

Another condition is persistence of the cell response to the input signal. In other words, the cell must function in an integrating manner. This feature further negates the quantum properties of the radiation flow and ensures the analog type of the cell interaction with optical radiation [22–24]. The condition is met by proteins found in cells that perform both analog and binary signal processing (including proteins contained in ganglion cells).

The last essential condition is that cells with an optical radiation-sensitive protein produce an analog response to variations in spatial, temporal, and energy analog-type parameters of external influences, responding with monotonically changing reversible cell-membrane depolarization [27–29]. The response is possible only for cells that perform analog signal processing and have preserved the simplest methods of receiving and processing the input signals in their phylogeny; i.e., these are rods, cones, and horizontal and bipolar cells [21, 29].

It naturally follows from the above that the conclusion that melanopsin is a molecule that converts optical signals in ipRGCs [1–3, 8] is true only in terms of the two first conditions; i.e., cells have an optical radiation-sensitive protein and function in an integrating manner.

Ganglion cells are incapable of receiving and processing the monotonically changing analog-type optical signals; they function on the trigger principle and process and generate only binary signals. Although optical radiation-sensitive proteins occur in their cytoplasm, this inability makes it impossible to believe that ganglion cells may act as receivers of optical radiation.

It should be noted again that melanopsin is believed to be sensitive to light of the short-wave range of the visible spectrum and to have a maximum at $\lambda = 440–460$ nm [1–3, 8]; however, there is still no reference to a study that would directly demonstrate the melanopsin sensitivity in the short-wave range of the visible spectrum.

As long as such a demonstration is lacking, melanopsin cannot be identified as a sensitive agent of ipRGCs, in contrast to the results in [1–3, 8].

In the unlikely event of fatal damage to the total receptor layer of the retina, the photodetector function may formally be performed by other cells, but only those capable of analog signal processing, as mentioned above. These are bipolar and horizontal cells [21, 27–29]. However, no evidence for a photodetector function of these cells has been obtained in several hundreds of years of studies of the retina. It is possible that such data are missing because the relevant proteins of bipolar and horizontal cells have extremely low sensitivity in the visible region of the optical spectrum or are sensitive to radiation outside the visible region.

The above arguments apparently lead to the conclusion that ganglion cells of the retina are basically incapable of functioning as photodetectors. Ganglion cells perform only the well-known function of associating transmitting units, which transform the input

signals into binary form, as in visual circuitry. In this sense, ganglion cells are intermediate elements in the pathway that controls and regulates the secretory activity of the pineal gland during the day and the circadian activity of the body.

All these circumstances and an analysis and additional mathematical processing of the data reported in [1–3, 8] allow an alternative and more natural interpretation of the data. The interpretation fully agrees with the current views of the function of retinal neuronal elements and controverts the existence of early unknown photodetectors, in particular, ipRGCs.

It is important to note that the interpretation proposed here directly follows from experimental findings in [1–3, 8] and by no means contravenes them.

The pathway that regulates circadian activity and the well-understood visual pathway function on the same principles evolved during phylogeny and utilize the same signal processing mechanisms and the same neuronal elements.

A certain set of rods and cones is assumed to act as photodetectors in the circadian activity-regulating pathway. These cells are in the peripheral region of the retina and converge to a few specialized ganglion cells with large receptive fields.

Given that similar principles underlie the processing of optical radiation in the circadian activity-regulating and visual pathways, the RCSEF for the former, like the relative spectral luminous efficiency functions for photopic ($V(\lambda)$) and mesopic ($V'(\lambda)$) vision, can be written as a normalized linear combination of the relative spectral-sensitivity functions of several types of photodetectors [17–19, 30]:

$$c(\lambda) = \frac{\sum_i \alpha_i \varphi_i(\lambda)}{\left[\sum_i \alpha_i \varphi_i(\lambda)\right]_{\max}}, \quad (1)$$

where $\varphi_i(\lambda)$ is the relative spectral-sensitivity function of the i-th photodetector type and α_i is the weighting factor that characterizes the contribution of the i-th photodetector type to the RCSEF formation.

The relative spectral-sensitivity functions $\varphi_i(\lambda)$ of the known photodetector types follow Gaussian functions that are symmetric about the respective mathematical expectations and monotonic in the short-wave and long-wave regions [30]:

$$\varphi_i(\lambda) \approx k_i \frac{1}{\sigma_i\sqrt{2\pi}} \exp\left[-\frac{(\lambda - \lambda_{i\max})^2}{2\sigma_i^2}\right], \quad (2)$$

where k_i is the normalizing factor, and $\lambda_{i\max}$ and σ_i are, respectively, the mathematical expectation and the mean square deviation of λ_i from $\lambda_{i\max}$ for the i-th photodetector.

An analysis of the $c_B(\lambda)$ and $c_T(\lambda)$ plots [1–3, 8] shown in Fig. 1 shows an important feature of their shapes; i.e., the functions are distinctly nonmonotonic in the long-wave range. The fact that the two functions are both nonmonotonic and clearly similar in the long-wave range indicates that the feature observed for $c_B(\lambda)$ and $c_T(\lambda)$ is a basic property of a RCSEF rather than a result of a technical or another experimental error.

A formal analysis of the nonmonotonic behavior in the long-wave range makes it possible to assume that two different photodetectors with the spectral sensitivity maximums $440 \le \lambda_{1\max} \le 450$ nm and $500 \le \lambda_{2\max} \le 520$ nm are involved in the formation of the functions $c_B(\lambda)$ and $c_T(\lambda)$.

With two photodetector types whose spectral sensitivities follow Eq. (2), Eq. (1) can be written as

$$c(\lambda) \approx \alpha_1 \frac{k_1}{\sigma_1\sqrt{2\pi}} \exp\left[-\frac{(\lambda - \lambda_{1\max})^2}{2\sigma_1^2}\right] + \alpha_2 \frac{k_2}{\sigma_2\sqrt{2\pi}} \exp\left[-\frac{(\lambda - \lambda_{2\max})^2}{2\sigma_2^2}\right]. \quad (3)$$

The fact that two terms form the sum in Eq. (3) indicates that two channels are used to regulate circadian activity in the retino-hypothalamic pathway. The photodetectors of the channels receive optical radiation in the shorter-wavelength (the first term in Eq. (3)) and longer-wavelength (the second term in Eq. (3)) spectral ranges.

The spectral characteristics of the photodetectors that form the function $c(\lambda)$ were established for $c_B(\lambda)$ and $c_T(\lambda)$ separately, using the experimental data reported in [1–3, 8]. The data were processed using the Graphical Analysis 3.1 program.

Because data on the behavior in the short-wave range have not been reported for $c_B(\lambda)$ and $c_T(\lambda)$ and a Gaussian function describes the spectral sensitivity of retinal photodetectors (3) [30], the corresponding regions of the functions were obtained by extrapola-

The parameters of the functions $c_1(\lambda)$ and $c_2(\lambda)$, which approximate the experimental functions $c_B(\lambda)$ and $c_T(\lambda)$

RCSEF	Shorter-wavelength term in Eq. (3)			Longer-wavelength term in Eq. (3)		
$c_i(\lambda)$	$\alpha_1 k_1$, nm	σ_1, nm	$\lambda_{1\max}$, nm	$\alpha_2 k_2$, nm	σ_2, nm	$\lambda_{2\max}$, nm
$c_1(\lambda)$	72.56	28.99	445	25.89	21.21	509
$c_2(\lambda)$	77.88	31.11	445	19.87	23.33	513

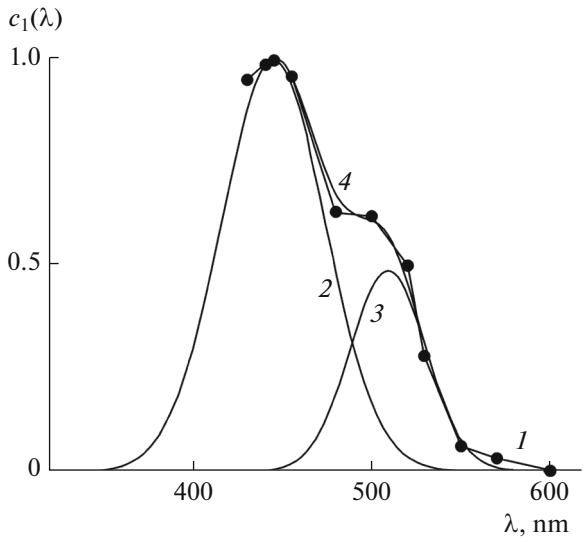

Fig. 2. Approximation of the function $c_B(\lambda)$: *1*, plot of the experimental function $c_B(\lambda)$; *2* and *3*, plots of the shorter- and longer-wavelength terms in Eq. (3); and *4*, plot of the function $c_1(\lambda)$, which approximates $c_B(\lambda)$.

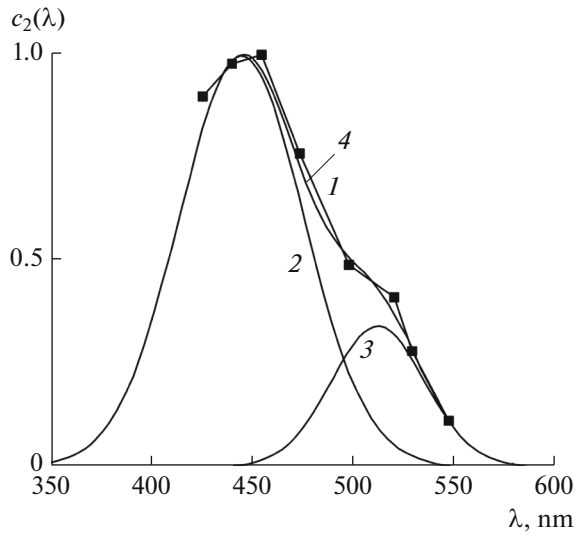

Fig. 3. Approximation of the function $c_T(\lambda)$: *1*, plot of the experimental function $c_T(\lambda)$; *2* and *3*, plots of the shorter- and longer-wavelength terms in Eq. (3); and *4*, plot of the function $c_2(\lambda)$, which approximates $c_T(\lambda)$.

tion using the Gaussian core of Graphical Analysis 3.1 in an automated mode and data established for the long-wave regions of the functions by the program. The approximation functions $c_1(\lambda)$ and $c_2(\lambda)$ were tested for fitting the experimental functions $c_B(\lambda)$ and $c_T(\lambda)$ by estimating the minimum mean square error of approximation.

The parameters $\alpha_1 k_1$, σ_1, $\lambda_{1\,max}$, $\alpha_2 k_2$, σ_2, and $\lambda_{2\,max}$ of the approximation functions $c_1(\lambda)$ and $c_2(\lambda)$ for Eq. (3) based on the experimental functions $c_B(\lambda)$ and $c_T(\lambda)$ are summarized in the table.

With the values shown in the table, the mean square error of the approximation was no more than 0.038 in the case of $c_B(\lambda)$ and no more than 0.068 in the case of $c_T(\lambda)$.

Plots of the experimental function $c_B(\lambda)$, its approximation function $c_1(\lambda)$, and the functions that describe its shorter- and longer-wavelength components are shown in Fig. 2. Similar plots obtained for the experimental function $c_T(\lambda)$ are shown in Fig. 3.

As is seen from Figs. 2 and 3, a nearly perfect coincidence of the plots was achieved between $c_B(\lambda)$ and $c_1(\lambda)$ and between $c_T(\lambda)$ and $c_2(\lambda)$ when $c_B(\lambda)$ and $c_T(\lambda)$ were approximated with $c_1(\lambda)$ and $c_2(\lambda)$ according to Eq. (3) with the parameter values shown in the table.

To identify the photodetector types corresponding to the functions $c_1(\lambda)$ and $c_2(\lambda)$, the table data were used, and the spectral-sensitivity functions following the shorter- and longer-wavelength terms of $c_1(\lambda)$ and $c_2(\lambda)$ in Eq. (3) were compared with the spectral-sensitivity functions of known retinal photodetectors.

The parameters $\lambda_{1\,max} = \lambda_{2\,max} = 445$ nm make it possible to assume that blue-sensitive cones with a spectral sensitivity maximum at $\lambda_{max} = 445$ nm are involved in the formation of the shorter-wavelength terms of the functions $c_1(\lambda)$ and $c_2(\lambda)$.

The normalized (to unity) spectral-sensitivity function $\varphi_{con}(\lambda)$ of the blue-sensitive cones is as follows [30]:

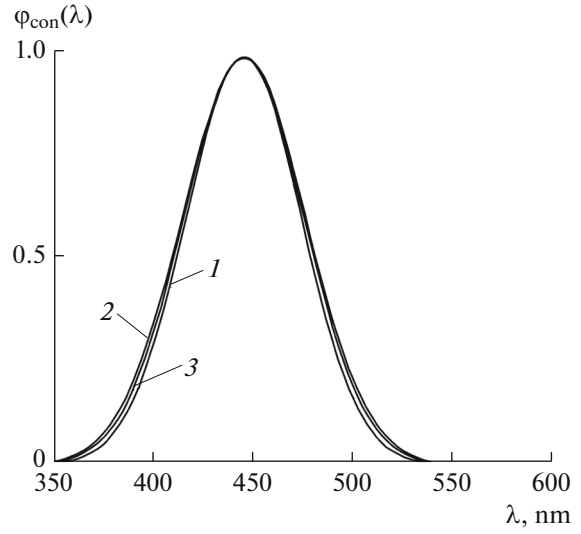

Fig. 4. *1* and *2*, normalized functions of the shorter-wavelength terms in Eq. (3) as obtained using data from [1] and [3], respectively; *3*, plot of the function $\varphi_{con}(\lambda)$ following Eq. (4).

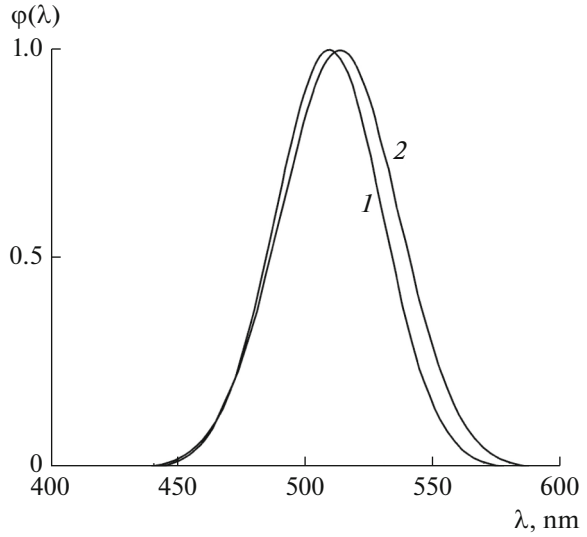

Fig. 5. *1* and *2*, normalized functions of the longer-wavelength terms in Eq. (3) as obtained using data from [1] and [3], respectively.

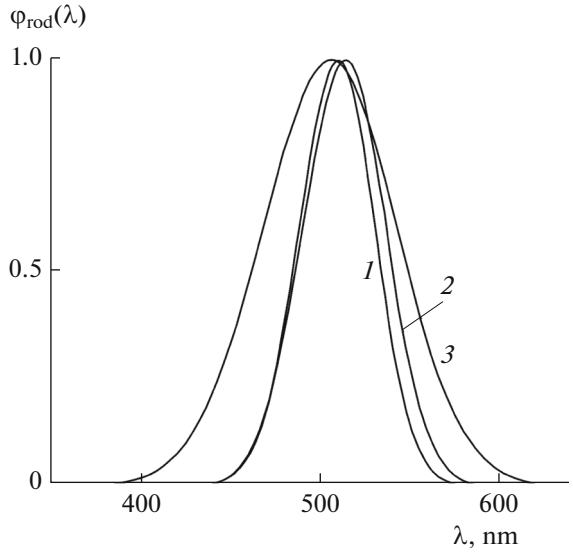

Fig. 6. *1* and *2*, normalized functions of the longer-wavelength terms of the functions $c_1(\lambda)$ and $c_2(\lambda)$, respectively; *3*, normalized spectral-sensitivity function $\varphi_{rod}(\lambda)$ of rods.

$$\varphi_{con}(\lambda) = 76.18\frac{1}{30.40\sqrt{2\pi}}\exp\left[-\frac{(\lambda-445)^2}{2\cdot 30.40^2}\right], \quad (4)$$

where the coefficient $k_{con} = 76.18$ is the normalizing factor, and $\sigma_{con} = 30.40$ is the mean square deviation.

Plots of the normalized (to unity) shorter-wavelength terms of the functions $c_1(\lambda)$ and $c_2(\lambda)$ and the normalized function $\varphi_{con}(\lambda)$ of blue-sensitive cones are shown in Fig. 4.

A comparison shows that the normalized shorter-wavelength terms of $c_1(\lambda)$ and $c_2(\lambda)$ fully coincide with the spectral-sensitivity function $\varphi_{con}(\lambda)$ of the blue-sensitive cones, clearly indicating that a certain set of the blue-sensitive cones of the retina are involved in the formation of the shorter-wavelength terms of the functions $c_B(\lambda)$ and $c_T(\lambda)$.

The longer-wavelength terms of the functions $c_1(\lambda)$ and $c_2(\lambda)$ in Eq. (3) describe the spectral sensitivity of some well-known or previously unidentified photodetectors of the retina. Normalization was performed again for the longer-wavelength terms of the functions $c_1(\lambda)$ and $c_2(\lambda)$ to allow more convenient comparisons. The normalizing factors that brought the maximum values of the longer-wavelength terms of $c_1(\lambda)$ and $c_2(\lambda)$ to unity were $k_1 = 53.15$ and $k_2 = 58.46$, respectively. The values of σ_1, $\lambda_{1\,max}$, σ_2, and $\lambda_{2\,max}$ are given in the table. The plots of the resulting functions are shown in Fig. 5.

As seen from Fig. 5, the longer-wavelength terms of the functions $c_1(\lambda)$ and $c_2(\lambda)$ are highly similar not only in shape, but also in their numerical values. The wavelengths that correspond to the maximums of the longer-wavelength terms of $c_1(\lambda)$ ($\lambda_{2\,max} = 509$ nm) and $c_2(\lambda)$ ($\lambda_{2\,max} = 513$ nm) do not coincide with any wavelength corresponding to the maximum of a spectral-sensitivity function of retinal cones [17–19]. As in [1–3, 8], the result leads to the conclusion that the longer-wavelength terms of the functions $c_1(\lambda)$ and $c_2(\lambda)$ are not associated with any of the three cone types.

However, the fact that the functions $c_B(\lambda)$ and $c_T(\lambda)$ have been obtained in independent studies and the similarity in parameters between the longer-wavelength terms of $c_1(\lambda)$ and $c_2(\lambda)$ indicate that the functions characterize the same type of photodetector that actually exists in the retina.

The wavelengths that correspond to the sensitivity maximums ($\lambda_{2\,max} = 509$ nm and $\lambda_{2\,max} = 513$ nm) of the longer-wavelength terms of the functions $c_1(\lambda)$ and $c_2(\lambda)$, their function domains, which are in the spectral range from 400 to 600 nm, and the shapes of the functions shown in Fig. 5 actually agree with the respective characteristics of the relative spectral luminous-efficiency function $V^1(\lambda)$ of mesopic vision, which has a maximum at the wavelength $\lambda_{max} = 505$ nm [17–19]. The function $V^1(\lambda)$ is known to be the same as the relative spectral-sensitivity function $\varphi_{rod}(\lambda)$ of the rod component of the visual system: $\varphi_{rod}(\lambda) \equiv V^1(\lambda)$.

Minor differences in $\lambda_{2\,max}$ between the longer-wavelength components of the functions $c_1(\lambda)$ and $c_2(\lambda)$ and the difference of their $\lambda_{2\,max}$ values from $\lambda = 505$ nm of the function $\varphi_{rod}(\lambda) = V_1(\lambda)$ might be attributed to differences in experimental conditions, experimental procedures, and data-processing methods and possible experimental errors.

The function $\varphi_{rod}(\lambda) \equiv V^1(\lambda)$ was approximated using the Gaussian core of Graphical Analysis 3.1 to yield the following equation:

$$\varphi_{rod}(\lambda) \equiv V^1(\lambda) = 93.92\frac{1}{37.48\sqrt{2\pi}}\exp\left[-\frac{(\lambda-505)^2}{2\cdot 37.48^2}\right], \quad (5)$$

where the coefficient $k_{rod} = 93.92$ is the normalizing factor and $\sigma_{rod} = 37.48$ is the mean square deviation.

The mean square error that characterizes the accuracy of approximating the function $\varphi_{rod}(\lambda) \equiv V^1(\lambda)$ with Eq. (5) is no more than 0.031.

Figure 6 shows the plots of the normalized (to unity) longer-wavelength terms of the functions $c_1(\lambda)$ and $c_2(\lambda)$ and the plot of the normalized rod spectral-sensitivity function $\varphi_{rod}(\lambda)$ following Eq. (5).

Comparison shows that the wavelengths that correspond to the maximum of the functions nearly coincide (Fig. 6). Although there is a difference between the mean square deviation σ_2 values of $c_1(\lambda)$ and $c_2(\lambda)$ and σ_{rod} of $\varphi_{rod}(\lambda)$, the fact that the retina lacks photodetectors with λ_{max} similarly close to $\lambda = 505$ nm makes it possible to believe that the unidentified photodetector is a type of rod that has a mean square deviation σ value lower than the σ value of $\varphi_{rod}(\lambda)$. Rods that function at a higher retinal irradiance corresponding to daylight conditions have been detected in experimental studies [31–33].

Certain differences in parameters between the longer-wavelength terms of the functions $c_1(\lambda)$ and $c_2(\lambda)$ and the function $\varphi_{rod}(\lambda)$ may arise if fewer rods are involved in the formation of the longer-wavelength terms of $c_1(\lambda)$ and $c_1(\lambda)$ and if their sensitivities have a narrower wavelength spread around $\lambda_{max} = 505$ nm compared with $\varphi_{rod}(\lambda)$.

The set of retinal rods with a low mean square deviation that was isolated via mathematical processing of the experimental data reported in [1–3, 8] is involved exclusively in forming the RCSEF of the pathway that regulates circadian activity, but not in the function of the pathway that is responsible for vision.

Data on the rod type involved in RCSEF formation were lacking until recently, possibly because it was not until recently that Brainard et al. [1] and Thapan et al. [3] reported the first data on the spectral characteristics of the circadian activity-regulating pathway from their experimental studies. Moreover, it was basically impossible to characterize the RCSER in studies of the visual pathway because the experimental protocols that are available in the field are unsuitable for characterizing the circadian activity-regulating pathway, which is highly specific and lacks any manifestation involved in vision.

It is clear that the function $c_1(\lambda)$, which approximates the data [1], shows a lower difference of $\lambda_{2\,max} =$ 509 nm of its longer-wavelength term from $\lambda_{max} =$ 505 nm, which corresponds to the maximum of the function $\varphi_{rod}(\lambda) \equiv V^1(\lambda)$ (5). The mean square error of approximation is also lower in the case of $c_1(\lambda)$. Hence, this function agrees far better with the current views of the spectral characteristics of retinal photodetectors as compared with the function $c_2(\lambda)$.

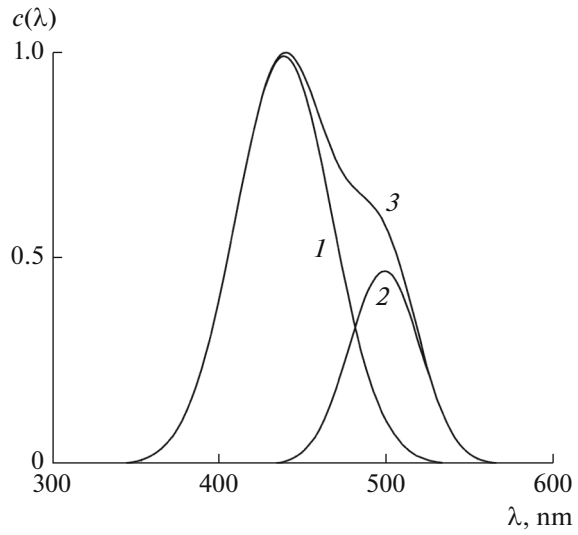

Fig. 7. RCSEF formed with participation of blue-sensitive cones and rods: *1* and *2*, plots of the shorter- and longer-wavelength terms of Eq. (7), respectively; *3*, plot of the function $c(\lambda)$.

In any case, the above data make it possible to conclude that at the current state of RCSEF studies and available relevant results, it is expedient to consider the RCSEF as a superposition of the shorter-wavelength term of the function $c_1(\lambda)$ or $c_2(\lambda)$ and the longer-wavelength term of $c_1(\lambda)$ with its mean square deviation $\sigma_2 = 21.11$ nm (table). The wavelength $\lambda_{2\,max} =$ 509 nm should be changed to 505 nm, which corresponds to the maximum sensitivity of the total set of retinal rods.

With these changes, Eq. (3) for the RCSEF can be written as

$$c(\lambda) \approx 72.56\frac{1}{28.99\sqrt{2\pi}}\exp\left[-\frac{(\lambda-445)^2}{2\cdot 28.99^2}\right] + 25.89\frac{1}{21.21\sqrt{2\pi}}\exp\left[-\frac{(\lambda-505)^2}{2\cdot 21.21^2}\right], \quad (6)$$

where $\alpha_1 k_1 = 72.56$, $\sigma_1 = 28.99$ nm, $\lambda_{1\,max} = 445$ nm, $\alpha_2 k_2 = 25.89$, $\sigma_2 = 21.21$, and $\lambda_{2\,max} = 505$ nm. A more convenient form is

$$c(\lambda) \approx 0.99\exp\left[-\frac{(\lambda-445)^2}{1680.84}\right] + 0.47\exp\left[-\frac{(\lambda-505)^2}{899.73}\right], \quad (7)$$

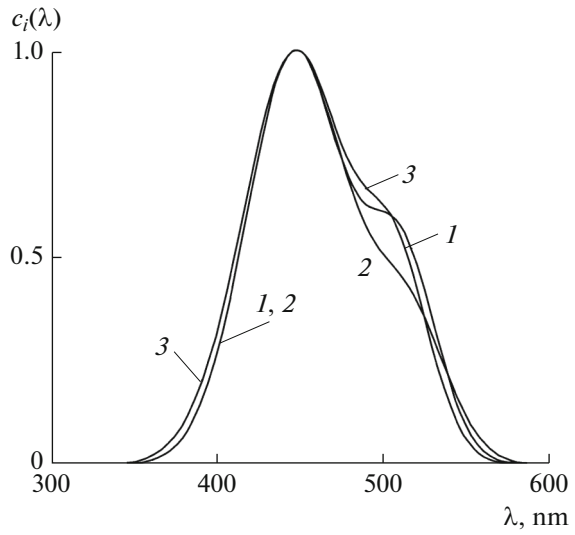

Fig. 8. *1* and *2*, functions $c_1(\lambda)$ and $c_2(\lambda)$, which approximates the experimental data [1] and [3], respectively; *3*, function $c(\lambda)$ formed with participation of rods and blue-sensitive cones.

where the coefficients 0.99 and 0.47 characterize the contributions of the shorter- and longer-wavelength channels of the retino-hypothalamic pathway in regulating circadian activity.

Figure 7 shows the plots of the shorter- and longer-wavelength terms and their sum $c(\lambda)$, which is the RCSEF that follows Eq. (7) and is formed with the participation of the well-known blue-sensitive cones and rods of the retina.

It is apparent from Eq. (7) and Fig. 7 that the shorter-wavelength channel of the retino-hypothalamic pathway plays a key role in regulating circadian activity; the channel is formed by blue-sensitive cones of the retina.

For comparison, Fig. 8 shows the plots of $c_1(\lambda)$ and $c_2(\lambda)$, which approximate the experimental data reported in [1, 3], and the plot of $c(\lambda)$ following Eq. (7).

As is seen from Fig. 8, the longer-wavelength part of the $c(\lambda)$ plot is similar in shape to $c_2(\lambda)$, but somewhat differs from the longer-wavelength part of $c_1(\lambda)$. Calculations show that the difference in shape between the functions $c_1(\lambda)$ and $c_2(\lambda)$ and the function $c(\lambda)$ is determined mostly by different contributions of rods in their formation and, consequently, different coefficients that modify the longer-wavelength term in Eq. (7). Far less important roles are played by the varying, but always minor differences in $\lambda_{2\,max}$, which corresponds to the maximum in the respective functions, and insignificant differences in the mean square deviation σ_2.

The fact that $c_1(\lambda)$ and $c_2(\lambda)$ differ from $c(\lambda)$ and that only a few experimental studies have focused on the RCSEF character indicate that additional experiments are necessary in order to determine the parameters of the functions $c_B(\lambda)$ and $c_T(\lambda)$ with shorter sampling intervals on the horizontal axis. Such experiments will help to more accurately estimate the coefficients and mean square deviations for the longer-wavelength term of Eq. (6) and the contributions of blue-sensitive cones and rods to the formation of the RCSEF following Eq. (7).

A review of the published data showed that Eq. (7) is currently the only analytical equation that allows a mathematical simulation of RCSEF-based processes, in particular, the regulation of the secretory activity of the pineal gland during the day, the regulation of human circadian activity, etc.

Thus, the above reasoning, the arguments, and the mathematical processing of data from the independent experimental studies [1–3, 8] provide well-grounded evidence that rods and blue-sensitive cones of the retina act together to form the RCSEF. These retinal elements act as receivers of optical radiation in the neuronal pathway that regulates the neuroendocrine system and eventually ensure the regulation of circadian activity. The findings that the two photodetector types perform a joint function, which is described by the two terms in Eq. (3), and that two spectral channels, that is, shorter- and longer-wavelength channels, act in the retino-hypothalamic pathway to regulate circadian activity indicate that the human regulation of melatonin secretion and circadian activity by optical radiation is far more intricate than described in the literature.

Regarding the so-called ipRGCs, the above data testify that these cells are incapable of receiving optical radiation and play no role in forming the RCSEF. Like all retinal ganglion cells, ipRGCs act as output elements of the retina and intermediate elements of the specialized pathway that regulates circadian activity. The cells perform only the well-known functions of integrating and transmitting binary signals to the hypothalamic suprachiasmatic nuclei and further neuronal structures associated with the pineal gland.

REFERENCES

1. G. C. Brainard and G. L. Glickman, CIE **152**, 1 (2003).
2. G. C. Brainard and G. L. Glickman, Svetotekhnika No. 1 (2004).
3. K. Thapan, J. Arendt, and D. J. Skene, J. Physiol. **535**, 261 (2001).
4. R. G. Foster, I. Provencio, D. Hudson, et al., J. Comp. Physiol. A **169**, 39 (1991).
5. M. S. Freedman, R. J. Lucas, B. Soni, et al., Science **284**, 502 (1999).
6. C. A. Czeisler, T. L. Shanahan, E. B. Klerman, et al., N. Engl. J. Med. **332**, 6 (1995).
7. E. B. Klerman, T. L. Shanahan, D. J. Brotman, et al., J. Biol. Rhythms **17**, 548 (2002).

8. G. C. Brainard and I. Provencio, in *Proc. 2nd CIE Expert Symposium on Lighting and Health (CIE 031*) (Vienna, 2006), pp. 6–21.
9. I. Provencio, G. Jiang, W. J. De Grip, et al., Proc. Natl. Acad. Sci. U. S. A. **95**, 340 (1998).
10. I. Provencio, I. R. Rodriguez, G. Jiang, et al., J. Neurosci. **20**, 600 (2000).
11. J. J. Gooley, J. Lu, T. C. Chou, et al., Nat. Neurosci. **4**, 1165 (2001).
12. D. M. Berson, F. A. Dunn, and M. Takao, Science **295**, 1070 (2002).
13. S. Hattar, H.-W. Liao, M. Takao, et al., Science **295**, 1065 (2002).
14. L. P. Morin, J. H. Blanchard, and I Provencio, J. Comp. Neurol. **465**, 401 (2003).
15. P. J. Sollars, C. A. Smeraski, J. D. Kaufman, et al., Vis. Neurosci. **20**, 601 (2003).
16. G. C. Brainard, J. P. Hanifin, J. M. Greeson, et al., J. Neurosci. **21**, 6405 (2001).
17. V. V. Meshkov and A. B. Matveev, *Foundations of Lighting Engineering*, Part 2: *Physiological Optics and Colorimetry*, 2nd ed. (Energoatomizdat, Moscow, 1989) [in Russian].
18. S. V. Kravkov, *The Eye and Its Functioning* (USSR Acad. Sci., Moscow—Leningrad, 1950) [in Russian].
19. V. Adrian, Svetotekhnika No. 1 (2009).
20. P. Berge, Y. Pomeau, and C. Vidal, L'ordre dans le chaos (Hermann, Editeurs des sciences et des arts, 1988).
21. F. Bloom, A. Lazerson, and L. Hofstadter, *Brain, Mind, and Behavior* (W. H. Freeman, New York, 1984; Mir, Moscow, 1988).
22. E. G. Pestov and G. M. Lapshin, *Quantum Electronics* (Voenizdat, Moscow, 1972) [in Russian].
23. R. M. Gagliardi and Sh. Karp, *Optical Communications* (Wiley, 1976; Scyaz', Moscow, 1978).
24. *Quantum Optics and Radiophysics: Lectures in Summer School on Theoretical Physics, Les Houches, France*, Ed. by O. V. Bogdankevich and O. N. Krokhin (Mir, Moscow, 1966) [in Russian].
25. V. M. Fain and Ya. I. Khanin, *Quantum Radiophysics* (Sovetskoe Radio, Moscow, 1965) [in Russian].
26. B. R. Levin and V. Schwarz, *Probabilistic Models and Methods in Communications and Control Systems* (The Statistical Theory of Communications, Vol. 24) (Radio i Svyaz', Moscow, 1985) [in Russian].
27. V. D. Glezer, *Sight and Mind* (Nauka, Leningrad, 1985) [in Russian].
28. F. B. Kogan, N. P. Naumov, V. G. Rezhabek, and O. G. Chorayan, *Biological Cybernetics* (Vysshaya Shkola, Moscow, 1972) [in Russian].
29. Yu. A. Trifonov, in *Sensory Systems: Vision* (Nauka, Leningrad, 1982) [in Russian].
30. A. V. Leonidov, Svetotekhnika No. 5, 49 (2010).
31. I. Abramov and J. Gordon, J. Optic. Soc. Am. **67** (2), 202 (1977).
32. B. Stabell and U. Stabell, J. Optic. Soc. Am. **70** (6), 706 (1980).
33. B. Stabell and U. Stabell J. Optic. Soc. Am. **71**, 841 (1981).

Translated by T. Tkacheva